

Angle-resolved photoemission spectroscopy study of the superconducting gap anisotropy in $\text{Bi}_2\text{Sr}_2\text{CaCu}_2\text{O}_{8+x}$

H. Ding

*Materials Sciences Division, Argonne National Laboratory, Argonne, Illinois 60439
and Department of Physics, University of Illinois at Chicago, Chicago, Illinois 60607*

M. R. Norman

Materials Sciences Division, Argonne National Laboratory, Argonne, Illinois 60439

J. C. Campuzano

*Materials Science Division, Argonne National Laboratory, Argonne, Illinois 60439
and Department of Physics, University of Illinois at Chicago, Chicago, Illinois 60607*

M. Randeria

Tata Institute of Fundamental Research, Bombay 400005, India

A. F. Bellman

*Materials Sciences Division, Argonne National Laboratory, Argonne, Illinois 60439
and Dipartimento di Fisica, Università di Milano, 20133 Milano, Italy*

T. Yokoya and T. Takahashi

Department of Physics, Tohoku University, 980 Sendai, Japan

T. Mochiku and K. Kadowaki

National Research Institute for Metals, Sengen, Tsukuba, Ibaraki 305, Japan

(Received 6 August 1996)

We report measurements of the momentum dependence of the superconducting gap in $\text{Bi}_2\text{Sr}_2\text{CaCu}_2\text{O}_{8+x}$ with angle-resolved photoemission spectroscopy using a dense sampling of the Brillouin zone in the vicinity of the Fermi surface. In the Y quadrant of the zone, where there are no complications from ghost bands caused by the superlattice, we find a gap function consistent within error bars to the form $\cos(k_x) - \cos(k_y)$ expected for a d -wave order parameter. Similar results are found in the X quadrant with the photon polarization chosen to enhance main band emission over that due to ghost bands. [S0163-1829(96)52238-1]

The past few years have seen an intense effort on the part of the condensed-matter physics community to determine the form of the order parameter in the high-temperature cuprate superconductors.¹ Part of this effort has relied on the use of high-resolution angle-resolved photoemission spectroscopy (ARPES) since this is the only known technique which can directly map out the momentum dependence of the superconducting gap.²⁻⁵

Very recently there has been considerable progress in ARPES studies of the cuprates. This includes evidence for a spectral function interpretation of ARPES via the study of sum rules,⁶ a detailed study of the Fermi surface,⁷ and momentum distribution⁸ in $\text{Bi}_2\text{Sr}_2\text{CaCu}_2\text{O}_{8+x}$ ($\text{Bi}2212$), and an elucidation of the polarization selection rules^{7,9} in the presence of the structural superlattice, which necessarily affects ARPES data on the highest quality $\text{Bi}2212$ samples. All these points are crucial in accurately determining the momentum dependence of the gap.

Modeling the experimental data in terms of spectral functions gives a quantitative estimate of the gap⁵ at a given location on the Fermi surface, but perhaps even more importantly, it provides a framework within which one can think about the data. This points to the importance of having a

very fine momentum space grid for data, and also for a very precise determination of the Fermi surface, in the neighborhood of the region where nodes in the gap occur. Further, the complications⁹ arising from the superlattice make it simplest to study the gap anisotropy in the Y quadrant,¹⁰ since here the main CuO Fermi surface is widely separated from the “ghost” Fermi surfaces due to the superstructure.¹¹

In this paper, we summarize the results obtained on several samples of $\text{Bi}2212$ with experiments which were designed taking into account all of the points listed above. We find that, within error bars, the excitation gap on the main Fermi surface sheet is consistent with $|\cos(k_x) - \cos(k_y)|$, as suggested by the earlier work of Ref. 3. The ARPES experiment cannot of course measure the phase of the order parameter, but this result is strongly suggestive of a $d_{x^2-y^2}$ order parameter. Finally, in order to prove that the two node gap previously seen in the X quadrant⁵ was indeed an artifact⁹ of the superstructure, we also study the X quadrant using a polarization geometry which enhances the main band relative to the “ghost” band, and obtain results which are in agreement with the Y quadrant.

The experiments were done at the Synchrotron Radiation Center, Wisconsin, using a high-resolution 4-m normal inci-

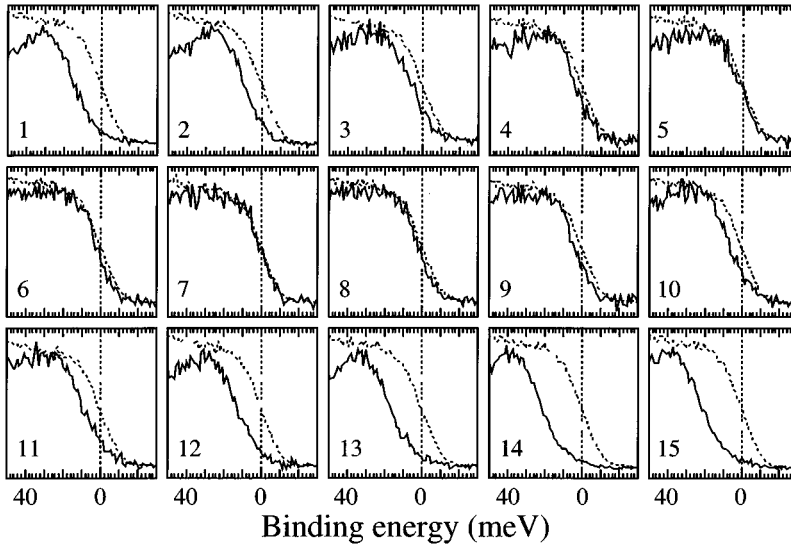


FIG. 1. Bi2212 spectra (solid lines) for a 87-K T_c sample at 13 K and Pt spectra (dashed lines) versus binding energy (meV) along the Fermi surface in the Y quadrant, with locations shown in Fig. 2.

dence monochromator with a resolving power of 10^4 at 10^{11} photons/s. We used 22-eV photons, with a 17-meV (full width at half maximum) energy resolution, and a momentum window of radius 0.045π (in units¹⁰ of $1/a^*$).

The crystals, which were grown by the traveling solvent floating zone method with an infrared mirror furnace, have low defect densities with structural coherence lengths ~ 1250 Å obtained from x-ray diffraction. The samples were cleaved *in situ* at 13 K in a vacuum of $< 5 \times 10^{-11}$ Torr. Most samples have very flat surfaces after cleaving, as measured by specular laser reflections. A flat surface is crucial for this experiment since it directly affects the momentum resolution. Another measure of the sample quality is the observation of the “ghost” bands due to the superlattice distortion; in our best sample (87-K T_c , with a 1-K transition width) we have now also seen evidence for the second umklapps from the superlattice. We will also present data from three other samples with a 90-K T_c .

In Fig. 1, we show the 13-K experimental energy distribution curves (EDC’s) for the 87-K T_c sample for various locations on the main band Fermi surface (FS) in the Y quadrant. The spectra shown correspond to the minimum observable gap along a set of \mathbf{k} points normal to the FS (for a detailed discussion of this in the context of a study of particle-hole mixing, see Ref. 8). These spectra are obtained from a dense sampling of \mathbf{k} space in the vicinity of the FS which is almost five times denser than previous data. In Ref. 5 a \mathbf{k} -step size of 0.064π normal to the FS and 0.064 – 0.081π along the FS was used in the Y quadrant (the radius of the \mathbf{k} window is 0.045π). The problem is that the bands are highly dispersive along ΓY with an energy change of about 85 meV per 0.064π step, and thus \mathbf{k}_F cannot be located accurately. Therefore, in our new measurements, we use a step size of 0.0225π normal to the Fermi surface and 0.045π along the Fermi surface. This not only allows us to map out the nodal region more clearly, but also improves by a factor of about 3 our ability to locate that spectrum whose binding energy at the center of the momentum window is closest to the Fermi energy (that is, the step size normal to the Fermi surface now corresponds to a dispersion of about 30 meV per step). In addition, at each \mathbf{k} point the

photon polarization is chosen along ΓX so as to maximize emission on the ΓY diagonal direction, i.e., $\Gamma Y \perp$ geometry (a polarization rotated 45° relative to this was used in Ref. 5).

In each panel of Fig. 1 we also plot the spectrum of a platinum reference, in electrical contact with Bi2212, measured periodically to determine the chemical potential, and to check for drifts in beam energy. (The polycrystalline Pt spectrum is a weighted density of states whose leading edge is an energy-resolution limited Fermi function.) The simplest gap estimate is obtained from the midpoint shift of the leading edge of Bi2212 relative to Pt. This has no quantitative validity (since the Bi2212 EDC is a spectral function,⁶ while Pt is a density of states) but yields an angular dependence which is qualitatively similar to the results described below.

The simplest way to quantitatively estimate the gap is to model⁵ the data in terms of a simple BCS line shape formula, taking into account the measured energy dispersion and the known energy and momentum resolutions. Two important points need to be discussed in connection with such fits: first, the lack of knowledge about the spectral line shape, especially its incoherent part, and, second, the large background in Bi2212 whose origin is unclear. In the large gap region near the \bar{M} point, we see a linewidth (imaginary self-energy) collapse, for frequencies smaller than 3Δ , upon cooling well below T_c .^{6,7} Thus the coherent piece of the spectral function is modeled by the BCS line shape, with all of the incoherent part lumped together with the experimental background in so far as the fitting procedure is concerned. We also showed⁵ that it was self-consistent (though perhaps not unique) to make the same assumption in the small gap region; the much larger width of the EDC in the diagonal direction arising due to the \mathbf{k} resolution combined with the large dispersion.

The gaps extracted by fitting the spectra of Fig. 1 are shown in Fig. 2. We emphasize that since the gap is determined by fitting the resolution-limited leading edge of the EDC, it is relatively unaffected both by self-energy effects, and by the experimental background which cuts off at low frequencies. To check this, we have made an independent set of fits to the small gap data where we do not use any background fitting function, and only try to match the leading

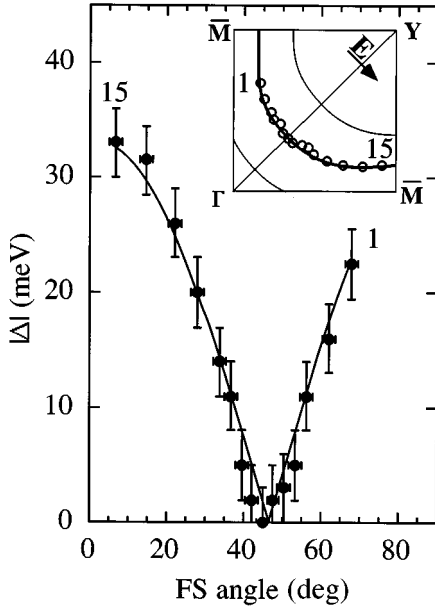


FIG. 2. Y quadrant gap in meV versus angle on the Fermi surface (filled circles) with fits to the data using a d -wave gap (solid curve). Labels of data points correspond to the spectra of Fig. 1. Inset shows their locations in the zone as well as the photon polarization direction.

edges, not the full spectrum. The two gap estimates are consistent within a meV. The (vertical) error bars of ± 3 meV on the gaps in Fig. 2 come primarily from the quality of the fit to the leading edge of the data and uncertainty in the location of the center of the \mathbf{k} window (near the diagonal direction), with smaller contributions coming from chemical potential determination (± 0.5 meV) and background modeling (± 0.5 meV). Horizontal error bars represent the accuracy in which we can determine the Fermi surface angle. This does not include any effective error bar coming from \mathbf{k} resolution, since this is in principle taken into account in the fits. The angular variation of the gap in Fig. 2 is in excellent agreement with that expected from a d -wave order parameter of the $\cos(k_x) - \cos(k_y)$ form.¹²

Next we turn to the X quadrant of the 87-K T_c sample. It is now recognized⁹ that the two node gap observed previously⁵ in the $\Gamma X||$ geometry came from an even linear combination of the ‘ghost’ bands due to the superlattice.¹¹ We thus choose the polarization along ΓY , so that on the diagonal we are in a $\Gamma X\perp$ geometry which enhances emission from the main band.¹³ The X quadrant gaps, determined from spectral function fits, are plotted in Fig. 3. We see that the hump in the gap along ΓX (45°) seen previously⁵ has indeed disappeared. The solid curve is a fit of the data to a d -wave gap function with a small sample misalignment (1.4° in real space). Note that for this data set, the step size along the Fermi surface was 0.135π and so is not dense enough around 45° to address the question of the detailed behavior around the node.

We next summarize the results (Fig. 4) for Y quadrant gaps extracted from fits on three different 90-K T_c samples. The main point is to note possible complications which arise in interpreting data sets which are not as dense in \mathbf{k} space as

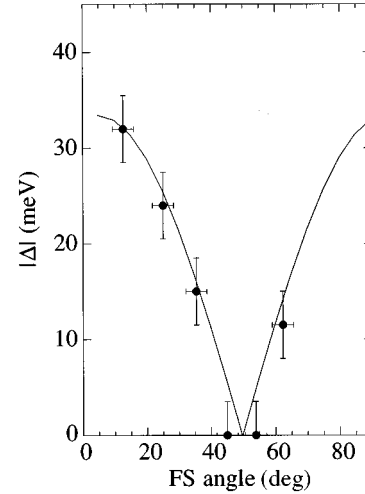


FIG. 3. X quadrant gap in meV, for the 87-K T_c sample, measured at 13 K, versus angle on the Fermi surface (filled circles) with fits to the data using a d -wave gap (solid curve). The photon polarization is along ΓY .

the detailed Y quadrant measurements on the 87-K sample described above (the step size along the Fermi surface being twice as large). The results on sample I have a region of reduced gap, consistent with zero, near 45° . To some extent this may be an artifact of the finite diameter of the \mathbf{k} window, which is 6° in FS angle.¹⁴ In addition, we found that for the small gap points of sample I the leading edge of the data lies above, i.e., to the right of, that of a zero gap spectral fit, assuming the \mathbf{k} window was centered at \mathbf{k}_F . We find that a combination of factors (\mathbf{k} -window center, chemical potential drift, and background) discussed above can indeed conspire to produce such an anomalous shift. These factors are already reflected in the ± 3 -meV error bars on the gap estimate, but we reiterate that the error bars must be borne in

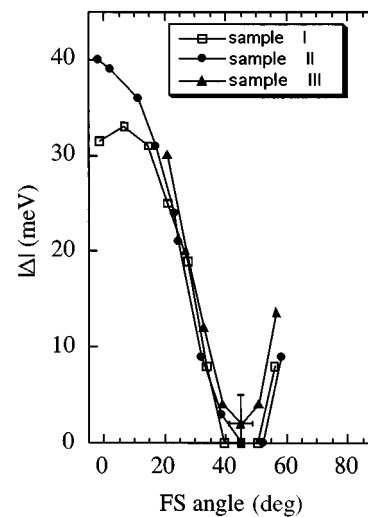


FIG. 4. Y quadrant gap in meV, measured at 13 K, versus angle on the Fermi surface for three different Bi2212 samples each with a 90-K T_c . For visual clarity only a representative error bar has been shown.

mind while interpreting the final results.

Similar issues arise with the results on sample II, and in addition both this and sample III appear to have an asymmetry about the diagonal (45°). For sample III, the asymmetry is quite large and almost certainly due to sample misalignment (of 1.8° in real space); the sample III results in Fig. 4 have been shifted by the corresponding FS angle to facilitate comparison with the other two samples. All of these caveats would also apply to the sparse Y quadrant data presented in Ref. 5, and, in particular, the shift of the node away from 45° in that data may also have been a consequence of sample misalignment.

In summary, we would say that the results of the 90-K samples are consistent, within error bars, with those obtained from the detailed measurements on the 87-K sample. There

is no hard evidence for either an extended region of nodes about 45° , or for a mixed symmetry gap.

In conclusion, we have determined the intrinsic momentum dependence of the superconducting gap in Bi2212 using dense momentum sampling of the zone in the vicinity of the Fermi surface. We find that the observed gap is consistent with the simple d -wave form¹⁵ $\cos(k_x) - \cos(k_y)$ within experimental error bars.

This work was supported by the U. S. Department of Energy, Basic Energy Sciences, under Contract No. W-31-109-ENG-38 and the National Science Foundation (DMR 91-20000) through the Science and Technology Center for Superconductivity and by Grant No. DMR-9624048. The Synchrotron Radiation Center is supported by NSF Grant No. DMR-9212658.

-
- ¹B. Goss-Levi, Phys. Today **49** (1), 19 (1996).
²C. G. Olson *et al.*, Science **245**, 731 (1989).
³Z.-X. Shen *et al.*, Phys. Rev. Lett. **70**, 1553 (1993).
⁴R. J. Kelley *et al.*, Phys. Rev. B **50**, 590 (1994).
⁵H. Ding *et al.*, Phys. Rev. Lett. **74**, 2784 (1995); **75**, 1425 (E) (1995).
⁶M. Randeria *et al.*, Phys. Rev. Lett. **74**, 4951 (1995).
⁷H. Ding *et al.*, Phys. Rev. Lett. **76**, 1533 (1996).
⁸J. C. Campuzano *et al.*, Phys. Rev. B **53**, 14 737 (1996).
⁹M. R. Norman *et al.*, Phys. Rev. B **52**, 15 107 (1995).
¹⁰We use a square lattice notation with the axes along the CuO bond directions. $X = (\pi, -\pi)$ and $Y = (\pi, \pi)$ in units of $1/a^*$, where $a^* = 3.83 \text{ \AA}$ is the separation between near-neighbor Cu ions. Thus the orthorhombic a axis is along X and b axis along Y .
¹¹The incommensurate superlattice in Bi2212 causes images (“ghost” bands) of the main CuO band. The first umklapps, always seen in good samples, are displaced from the main band by \pm the superlattice vector $\mathbf{Q} = (0.21\pi, 0.21\pi)$. In the Y quadrant, the bands and the corresponding Fermi surfaces are widely separated, since \mathbf{Q} is along ΓY ; however this is not so in the X quadrant; see Ref. 7 and M. R. Norman *et al.*, Phys. Rev. B **52**, 615 (1995).
¹²The actual functional form is $\cos(2\phi + \phi_0)$, where ϕ_0 , with a best fit value 1.4° (in FS angle), represents a possible sample misalignment (in real space) of $\approx 0.4^\circ$. This form agrees very closely with $\cos(k_x) - \cos(k_y)$ over the observed FS up to a multiplicative constant of 0.46.
¹³In principle an odd “ghost” band, with the same symmetry as the main band, should also contribute in this geometry (Ref. 9). There is, however, no evidence (Ref. 7) in the data for such an odd “ghost” band, possibly due to final state effects. We note that the emission intensities from the main and ghost bands are not well understood at this time.
¹⁴So as not to prejudice the fits, the gap was considered to be a constant within the momentum window. This condition is obviously violated in the d -wave case near the node where the gap is varying rapidly with momentum.
¹⁵Such an order parameter arises naturally from theories with antiferromagnetic spin fluctuations and/or strong correlations. For recent reviews, see D. Pines and P. Monthoux, J. Phys. Chem. Solids **54**, 1651 (1995); D. J. Scalapino, Phys. Rep. **250**, 329 (1995); J. Phys. Chem. Solids **56**, 1669 (1995).